

1 **RACK1 associates with RNA-binding proteins Vigilin and SERBP1 to**
2 **control dengue virus replication**

3

4 Alexis Brugier¹, Mohamed-Lamine Hafirassou¹, Marie Pourcelot¹, Morgane
5 Baldaccini², Laurine Couture¹, Vasiliya Kril¹, Beate M. Kümmerer³, Sarah Gallois-
6 Montbrun⁴, Lucie Bonnet-Madin^{1#}, Sébastien Pfeffer², Pierre -Olivier Vidalain⁵,
7 Constance Delaugerre^{1,6}, Laurent Meertens¹, Ali Amara^{1,&}

8

9 ¹ Université de Paris, INSERM U944 CNRS 7212, Biology of Emerging Viruses team,
10 Institut de Recherche Saint-Louis, Hôpital Saint-Louis, 75010 Paris, France

11 ² Université de Strasbourg, Architecture et Réactivité de l'ARN, Institut de Biologie
12 Moléculaire et Cellulaire du CNRS, 67084 Strasbourg, France

13 ³ Institute of Virology, Medical Faculty, University of Bonn, 53127 Bonn, Germany

14 ⁴ Université de Paris, Institut Cochin, INSERM, CNRS, F-750014 PARIS, France
15 Inserm U1016 - CNRS UMR8104 –75014 Paris

16 ⁵ Centre International de Recherche en Infectiologie (CIRI), Team Viral Infection,
17 Metabolism and Immunity, Univ Lyon, Inserm U1111, CNRS UMR5308, ENS de Lyon,
18 Université Claude Bernard Lyon 1, 69007 Lyon, France

19 ⁶ Laboratoire de Virologie et Département des Maladies Infectieuses, Hôpital Saint-
20 Louis, APHP, 75010 Paris, France

21

22 [#] Current address : Institut de Génétique Humaine, Laboratoire de Virologie
23 Moléculaire, CNRS-Université de Montpellier, 34000 Montpellier, France

24 [&] Corresponding author

25 **Abstract**

26 Dengue virus (DENV), a re-emerging virus transmitted by *Aedes* mosquitoes, causes
27 severe pathogenesis in humans. No effective treatment is available against this virus.
28 We recently identified the scaffold protein RACK1 as a component of the DENV
29 replication complex, a macromolecular complex essential for viral genome
30 amplification. Here, we show that RACK1 is important for DENV infection. RACK1
31 mediates DENV replication through binding to the 40S ribosomal subunit. Mass
32 spectrometry analysis of RACK1 partners coupled to a loss-of-function screen
33 identified the RNA binding proteins Vigilin and SERBP1 as DENV host dependency
34 factors. Vigilin and SERBP1 interact with DENV viral RNA (vRNA), forming a ternary
35 complex with RACK1 to mediate viral replication. Overall, our results indicate that
36 RACK1 recruits Vigilin and SERBP1, linking the DENV vRNA to the translation
37 machinery for optimal translation and replication.

38

39 Introduction

40 Dengue virus (DENV) belongs to the genus *Flavivirus* of the family *Flaviviridae*,
41 which includes important emerging and reemerging viruses such as West Nile virus
42 (WNV), yellow fever virus (YFV), Zika virus (ZIKV), and tick-borne encephalitis virus
43 (TBEV)¹. DENV is transmitted to human by an *Aedes* mosquito bite and may lead to
44 a variety of diseases ranging from mild fever to lethal dengue hemorrhagic fever and
45 dengue shock syndrome². Recent estimations indicate that half of the world's
46 population lives in areas where dengue fever is endemic³, with 100 million
47 symptomatic infections including 500,000 cases of severe manifestations of the
48 disease per year⁴. There are currently no approved antiviral therapies against DENV,
49 although a promising inhibitor targeting the viral NS3-NS4B interaction was recently
50 described⁵. Conversely, the recently approved tetravalent lived-attenuated vaccine
51 showed disappointing efficacy^{6,7}.

52 DENV is an enveloped virus containing a positive-stranded RNA genome of
53 ~11-kb. Upon entry into the host cell, the viral genome is released in the cytoplasm
54 and translated by the host machinery into a large polyprotein precursor that is
55 processed by host and viral proteases. Co- and post-translational processing gives
56 rise to three structural proteins, [C (core), prM (precursor of the M protein) and E
57 (envelope) glycoproteins] which form the viral particle and seven non-structural
58 proteins (NS) called NS1, NS2A, NS2B, NS3, NS4A, NS4B and NS5⁸ that play central
59 roles in viral genome replication, assembly and modulation of innate immune
60 responses⁹. Like other flaviviruses, DENV genome replication takes place within virus-
61 induced vesicles (Ve) derived from invaginations of the endoplasmic reticulum (ER)
62 membrane^{10,11}. These structures consist of 90 nm-wide vesicles containing a \pm 11 nm
63 pore allowing exchanges between the Ve lumen and the cytosol¹¹. Within the Ve, viral

64 NS proteins, viral RNA (vRNA), and some host factors assemble to form the viral
65 replication complex (RC) that is essential for viral RNA synthesis. We have recently
66 purified the DENV RC in human cells, using a tagged DENV subgenomic replicon, and
67 determined its composition by mass spectrometry ¹². Our study provided an
68 unprecedented mapping of the DENV RC host interactome and identified cellular
69 modules exploited by DENV during active replication. By combining these proteomics
70 data with gene silencing experiments, we identified a set of Host Dependency Factors
71 (HDFs) that critically impact DENV infection and established an important role for
72 Receptor for Activated C-Kinase 1 (RACK1) in DENV vRNA amplification ¹², which was
73 recently confirmed by others ¹³.

74 RACK1 is a core component of the 40S ribosomal subunit ^{14,15}, containing
75 seven WD40 domains that mediate protein / protein interactions ^{16,17}. RACK1 is a
76 scaffold protein ^{18,19} described to interact with many cellular pathways such as
77 Sarcoma (Src) tyrosine kinase ^{20,21}, cAMP/PKA ²² or receptor tyrosine kinase ²³.
78 Ribosomal RACK1 has also been shown to be involved in the association of mRNAs
79 with polysomes ²⁴, the recruitment and phosphorylation of translational initiation factors
80 ²⁵⁻²⁷ and in quality control during translation ²⁸. The non-ribosomal form of RACK1 is
81 involved in innate immunity, by recruiting the PP2A phosphatase ²⁹ or by targeting the
82 VISA/TRAF complexes ³⁰ and participates in the assembly and activation of the NLRP3
83 inflammasome ³¹. To date, only one proteomic study aiming to identify RACK1
84 cofactors has been performed in *Drosophila* S2 cells ³². RACK1 cellular partners in
85 human cells are largely unknown.

86 Several viruses depend on RACK1 to complete their infectious cycle ³¹⁻³⁵. For
87 instance, RACK1 is involved in IRES-mediated translation of viruses possessing a type
88 I IRES such as cricket paralysis virus or hepatitis C virus ³³. RACK1 also contribute to

89 poxvirus infection through a ribosome customization mechanism. Indeed, poxviruses
90 trigger the phosphorylation of the serine 278 of RACK1³⁴ to promote the selective
91 translation of viral RNAs .

92 In this work, we have investigated the function of RACK1 during DENV life cycle.
93 We performed the first interactome of RACK1 in human cells. Functional studies
94 revealed that RACK1 forms with the RNA binding proteins Vigilin and SERBP1 a
95 ternary complex that binds viral RNA to regulate DENV genome amplification.

96

97 **Results and discussion**

98

99 **RACK1 interaction with the 40S ribosomal subunit is required for DENV infection**

100 To confirm the role of RACK1 in DENV infection, we challenged parental and
101 RACK1 knockout (RACK1^{KO}) HAP1 cells with DENV2-16681 particles at different
102 multiplicity of infections (m.o.i) and measured viral infection by quantifying the
103 percentage of cells expressing the DENV antigen PrM. In agreement with our previous
104 studies ¹², DENV infection was severely impaired in HAP1 cells lacking RACK1 (Fig. 1
105 a, b). Importantly, *trans*-complementation of the HAP1 RACK1^{KO} cells with a plasmid
106 encoding human RACK1 rescued cell susceptibility to DENV infection (Fig. 1 a, b),
107 ruling out off-target effects and demonstrating that RACK1 is an important host factor
108 for DENV.

109 RACK1 is a component of the 40S subunit of the ribosome and is located in
110 near the mRNA exit channel ¹⁷. To test whether DENV infection requires RACK1
111 association with the 40S ribosome, we *trans*-complemented RACK1^{KO} cells with a
112 RACK1 mutant defective for ribosome-binding (RACK1R36D/K38E, DE mutant) ^{34,35} .
113 The RACK1 DE mutant which displayed WT expression level and was unable to
114 associated with polysomes (supplementary Fig.1), as previously described ³⁶ and,
115 importantly failed to rescue DENV2-16681 infection (Fig. 1 c, d). These results indicate
116 that the interaction with the 40S ribosomal subunit is important for RACK1 proviral
117 function.

118

119 **Mapping the RACK1 interactome**

120 Because RACK1 is a scaffold protein, we hypothesized that its proviral activity
121 may rely on its ability to recruit host proteins near the ribosome for optimal translation.

122 To characterize the RACK1 interactome in mammalian cells, we transfected 293T cells
123 with a plasmid encoding an HA-tagged version of human RACK1. We pulled-down
124 RACK-1 and its binding partners using HA beads and eluated purified proteins with HA
125 peptide according to the experimental procedure that we recently described¹².
126 Immunoprecipitated proteins were separated by SDS-PAGE, visualized by silver-
127 staining, and subjected to mass spectrometry (MS) analysis (Fig. 2a, supplementary
128 Fig. 2 a, b). By analyzing the raw AP-MS dataset with SAINT express and MiST
129 softwares ³⁷, we identified 135 high confidence host factors that co-purified with
130 RACK1 and showed a SAINT express score >0.8 (Table 1). Next, we analyzed the list
131 of 135 high-confidence interactors with DAVID 6.8 to identify statistical enrichments for
132 specific Gene Ontology (GO) terms from the “cellular component” (CC) annotation ^{38,39}
133 (Fig. 2b) and built the corresponding interaction network using Cytoscape 3.4.0 ⁴⁰ (
134 Fig.2c). The 135 RACK1- interacting proteins were clustered into functional modules
135 using enriched GO terms as a guideline and literature mining (Fig. 2c). As expected,
136 the RACK1 interactome was significantly enriched in proteins associated to
137 ribosome/polysome and mRNA translation (Rps3, EIF3, eIF4G, eIF4J), stress
138 granules (G3BP2, LARP1), P-Bodies (Ago1 and 2) and RNA splicing factors
139 (HNRNPA2B1, U2AF2) (Fig. 2c).

140 **Vigilin, SERBP1 and ZNF598 are DENV host dependency factors**

141 To pinpoint the function of the RACK-1 binding partners during DENV infection,
142 we silenced by RNA interference (RNAi) the expression of the 49 highest ranked hit
143 with an average peptide count >28 , (Fig. 3a, supplementary Fig. 2c) and determined
144 the consequences on viral infection (Fig. 3a, supplementary Fig. 3a, Table 2). Four
145 proteins, namely HNRNPA2B1, Vigilin, SERBP1 and ZNF598 whose silencing
146 decreased infection by at least 50% without affecting cell viability in the two cell lines

147 were considered for further investigations (Fig. 3a, supplementary Fig. 3a, Table 2)
148 These factors are RNA-Binding Proteins (RBP) involved in RNA splicing
149 (HNRNPA2B1) ⁴¹ or translation regulation (Vigilin, SERBP1, ZNF598) ^{28,42,43}.
150 HNRNPA2B1 was already described to interact with the 3'UTR part of the virus ⁴⁴.
151 Because HNRNPA2B1 is a nuclear protein ⁴⁵, it was not further considered in our
152 study. Vigilin is a multiple K-homology (KH) domain protein implicated in translation
153 regulation and lipidic metabolism ^{24,43,46}. This protein was recently described to bind
154 the DENV RNA and, in association with the ribosomal-binding protein 1 (RRBP1), to
155 facilitate viral RNA translation and replication ⁴⁷. However, how this protein interacts
156 with RACK1 to regulate DENV infection is still unknown. SERBP1 is a RACK1 cofactor
157 ⁴⁸ that is located at the entry channel of ribosomes ⁴⁹ and enhances translation by
158 promoting the association of mRNAs with polysomes ⁴². SERBP1 was also described
159 to interact with DENV RNA, however its role in DENV replication remains unclear ⁵⁰.
160 Finally, ZNF598 is an E3 ubiquitin-protein ligase known to interact with RACK1 and
161 playing a key role in the ribosome quality control ²⁸. ZNF598 was also described to
162 play a role in innate immunity ⁵¹, however its role in DENV infection is unknown.

163 We first confirmed that endogenous Vigilin, ZNF598 and SERBP1 proteins co-
164 immunoprecipitated with HA-RACK1 ectopically expressed in 293T cells (Fig. 3b). Next
165 we validated the requirement of Vigilin, SERBP1 and ZNF598 using two approaches.
166 On one hand, we found that knocking-down by RNA interference Vigilin, SERBP1 or
167 ZNF598 significantly impaired DENV infection of primary human fibroblasts which are
168 DENV target cells (Supplementary Fig. 3b, c). On the other hand, we use the
169 CRISPRCas9 technology to edit the corresponding genes in HAP1 cells (Vigilin ^{KO},
170 SERBP1 ^{KO}, ZNF598 ^{KO}). Gene editing and knock-out generation were confirmed by
171 genomic DNA sequencing (Supplementary Fig. 3d) and western blot analysis

172 (Supplementary Fig. 3e), respectively. In agreement with our previous findings, lack of
173 RACK1, Vigilin, SERBP1 and ZNF598 expression had no impact on cell growth and
174 viability as assessed by quantification of ATP levels in culture wells at different
175 timepoints (Supplementary Fig. 3f). HAP1 cells lacking Vigilin, SERBP1 or ZNF598
176 expression were poorly permissive to DENV infection as shown by the quantification
177 of viral progeny in supernatants of infected cells (Fig. 3c), western blot analysis of the
178 DENV protein expression (NS3, E, PrM) (Fig. 3d), and quantification of the viral RNA
179 (Fig. 3e). Parental (Control) and HAP1 cells transfected with a non-specific gRNA
180 (sgGFP) were used as negative controls (Fig. 3) while RACK1^{KO} HAP1 cells as a
181 positive control (Fig. 3). We then investigated if these phenotypes were specific to
182 DENV2-16681 or could be observed with other flaviviruses. We found that Vigilin,
183 SERBP1 and ZNF598 mediate infection by other DENV serotypes (Supplemental Fig.
184 3g), as well as by Zika virus (ZIKV), a related flavivirus (Fig. 3f). In contrast, infections
185 by the alphavirus Chikungunya virus (CHIKV) or vesicular stomatitis virus G protein
186 (VSV-G)-pseudotyped Human Immunodeficiency Virus (VSVpp), were unaffected in
187 Vigilin^{KO} and SERBP1^{KO} cells (Fig. 3f). CHIKV infection but not VSVpp was
188 significantly reduced in RACK1^{KO} and ZNF598^{KO} cells (Fig. 3f). Altogether, our data
189 indicate that Vigilin, SERBP1 and ZNF598 are important host factors for DENV.
190 ZNF598 is required for DENV and CHIKV infection while Vigilin and SERBP1 are
191 exclusively exploited by DENV and other related flaviviruses.

192 **Vigilin and SERBP1 regulate DENV translation and replication**

193 To determine whether Vigilin and SERBP1 impact initial vRNA translation or
194 amplification, Vigilin^{KO} and SERBP1^{KO} cells were challenged with DENV2 *Renilla*
195 luciferase (Luc) reporter virus (DV-R2A) through a time-course experiment to monitor
196 the kinetic of viral infection (Fig. 4a). RACK1^{KO} cells were used as a positive control.

197 A small peak of the Luc activity was detected at 6 hr post-infection, reflecting the initial
198 translation of the incoming vRNA. This was followed by a marked increase in Luc
199 activity due to vRNA amplification (translation and replication) (Fig. 4a). Depletion of
200 RACK1, Vigilin and SERBP1 had no impact on initial translation step but strongly
201 impaired DENV vRNA amplification at later time-points (Fig. 4a). Importantly, viral
202 genome replication was completely restored in KO cells transduced with RACK1,
203 SERBP1 or Vigilin cDNAs (Fig. 4a and supplementary Fig. 4a). Consistent with Fig. 3f,
204 CHIKV expressing the Gaussia luciferase replicated as efficiently in Vigilin or SERBP1
205 ^{KO} cells than control cells while its replication in RACK1 ^{KO} was impaired (Fig. 4b). To
206 assess further the effect of Vigilin and SERBP1 on DENV vRNA replication, we used
207 a *Renilla* luciferase (Rluc) reporter sub-genomic replicon (sgDVR2A). This latter is a
208 self-replicating DENV RNA containing a large in-frame deletion in the structural genes
209 and represents a useful tool to exclusively monitor DENV translation and RNA
210 amplification. Control, Vigilin ^{KO}, SERBP1 ^{KO}, and RACK1 ^{KO} HAP1 cells were
211 transfected with the *in vitro*-transcribed DENVR2A sub-genomic RNA and vRNA
212 replication was monitored over time by quantifying the Rluc activity in infected cell
213 lysates (Fig. 4c). Depletion of RACK1, Vigilin or SERBP1 had no impact during the
214 early phase of DENV RNA translation. At 12h post-transfection, the RLuc signal
215 increased over time in control cells, while a strong reduction was observed (more than
216 10-fold reduction at 48 hpi) in Vigilin ^{KO} and SERBP1 ^{KO} cells (Fig. 4c). The RLuc signal
217 was restored in Vigilin ^{KO} or SERBP1 ^{KO} trans-complemented with their corresponding
218 cDNAs (Fig. 4c).

219 Vigilin has been previously shown to mediate, in association with the host factor
220 RRBP1, the stability of DENV vRNA ⁴⁷. Since SERBP1 also binds the DENV RNA ⁵⁰,
221 we reasoned that it might play a similar role. To assess this hypothesis RACK1^{KO},

222 Vigilin^{KO} or SERBP1^{KO} HAP1 cells where challenged with DENV followed by treatment
223 with MK0608 to inhibit viral replication ⁴⁵. Then, we monitored the decay of the vRNA
224 overtime by northern blot analysis using a probe that targets the DENV 3'UTR
225 (supplementary data Fig. 4b). We observed that the levels of the DENV genomic RNA
226 was similar in control, RACK1^{KO} and SERBP1^{KO} HAP1 cells up to 24 h after MK0608
227 treatment (supplementary data Fig. 4b). Surprisingly, lack of Vigilin expression had a
228 very mild effect on DENV RNA stability (supplementary data Fig. 4b). Together, these
229 results show that RACK1, Vigilin and SERBP1 promote viral replication without a major
230 impact on the stability of DENV vRNA.

231 **Vigilin and SERBP1 interactions with RACK1 are important for DENV infection**

232 Scp160p and Asc1p, the yeast homologs of Vigilin and RACK1 respectively,
233 have been shown to interact each other ²⁴. This interaction is thought to promote
234 translation of specific mRNAs linked to Scp160p by mediating their association with
235 polysomes ²⁴. Because Vigilin is very well-conserved amongst different species, a
236 similar interaction with RACK1 might occur in mammalian cells. Having established
237 that Vigilin and SERBP1 do not have a major influence on the stability of the vRNA,
238 we hypothesized that their proviral effect might be linked to their interaction with
239 RACK1. Previous studies showed that Scp160p interacts with Asc1p via the KH 13
240 and 14 domains located in its C-terminal region ⁵² while SERBP1 interacts directly with
241 RACK1 through a motif (aa 354 to 474) which contains the RGG domain ⁴⁸
242 (supplementary data Fig. 5a). On the bases of these observations, we generated the
243 corresponding deletion mutants of Flag-tagged Vigilin (Flag Vigilin Mut) and Myc-
244 tagged SERBP1 (Myc SERPB1 Mut) (supplementary data Fig. 5a)and test their ability
245 to interact with RACK1 (Fig. 5a, supplementary data Fig. 5). Pull-down experiments
246 showed that RACK1 binds both WT FLAG Vigilin or WT Myc SERBP1 ectopically

247 expressed in HEK-293T cells (Fig. 5a). In contrast, RACK1 failed to associate with
248 mutant forms of Vigilin and SERBP1 (Fig. 5a). Using an RNA-IP assay, we showed
249 that Vigilin Mut and SERBP1 Mut bound the DENV vRNA as the same extent as their
250 WT counterparts (Fig. 5b and supplementary Fig. 5b). Finally, infection studies showed
251 that expression of Mut Vigilin or Mut SERBP1 in Vigilin^{KO} or SERBP1^{KO} cells,
252 respectively, did not restore DENV2-16681 infection in contrast to their WT
253 counterparts (Fig. 5c, supplementary Fig. 5c). Together, these data indicate that the
254 ability of Vigilin and SERBP1 to bind RACK1 but not the vRNA is required for DENV
255 infection.

256

257 **Conclusions**

258 In this study, we performed the first RACK1 interactome in human cells and identified
259 Vigilin and SERBP1 as host factors for DENV infection. Both are RNA-binding proteins
260 that interact with the DENV RNA and regulate viral replication. Importantly, our data
261 suggest that Vigilin, SERBP1 and RACK1 form a ternary complex important for DENV
262 RNA amplification. The proviral function of RACK1 depends on its association with
263 the 40S ribosomal subunit. Furthermore, mutants of SERBP1 or Vigilin that lost their
264 ability to interact with RACK1 were unable to support infection. Overall, our results
265 provide new insights into the molecular mechanisms of DENV replication and indicate
266 that RACK1 acts as a binding platform at the surface of the 40S ribosomal subunit to
267 recruit Vigilin and SERBP1, which may therefore function as linkers between the viral
268 RNA and the translation machinery to selectively amplify DENV genome. Strategies
269 that interfere with RACK1-ribosome association or disturb the RACK1-Vigilin-SERBP1
270 complex may represent new ways to combat DENV-induced disease.

271

273

274 **Methods**

275 **Cell lines**

276 HAP1 cells (Horizon Discovery), and HAP1 RACK1^{KO} (provided by Dr Gabriele Fuchs;
277 University at Albany) were cultured in IMDM supplemented with 10% fetal bovine
278 serum (FBS), 1% penicillin–streptomycin, 1% GlutaMAX and 25 mM HEPES.
279 HEK293T (ATCC), Vero E6 (ATCC), BHK-21 (ATCC), HeLa (ATCC) cells were
280 cultured in DMEM supplemented with 10% FBS, 1% penicillin–streptomycin, 1%
281 GlutaMAX and 25 mM HEPES. Fibroblast BJ-5ta cells (ATCC) were cultured according
282 to the manufacturer’s instructions. A final concentration of 50 µM of MK0608 was used
283 in this study. All cell lines were cultured at 37°C and 5% CO₂.

284

285 **Virus strains and replicons.**

286 DENV1-KDH0026A (gift from L. Lambrechts, Pasteur Institute, Paris), DENV2-16681
287 (Thailand/16681/84), DENV4 (H241) and ZIKV HD78788 were propagated in mosquito
288 AP61 cell monolayers with limited cell passages. DENV2 Rluc reporter virus (DVR2A)
289 was provided by Ralf Bartenschlager (University of Heidelberg). The CHIKV Luc
290 reporter virus was described previously⁵³. To generate infectious virus, capped viral
291 RNAs were generated from the NotI-linearized plasmids using a mMessage
292 mMACHINE T7 Transcription Kit (Thermo Fisher Scientific) according to the
293 manufacturer’s instructions. RNAs were purified (see RNA IP protocol), resuspended
294 in Dnase/Rnase free water, aliquoted and stored at –80 °C until used. 30 µg of purified
295 RNAs were transfected in BHK21 cells using lipofectamine 3000 reagent.
296 Supernatants were collected 72 hrs later and used for viral propagation on Vero E6
297 cells. For all of the viral stocks used in flow cytometry experiments, viruses were

298 purified through a 20% sucrose cushion by ultracentrifugation at 80,000g for 2 h at 4
299 °C. Pellets were resuspended in HNE1X pH 7.4 (HEPES 5 mM, NaCl 150 mM, EDTA
300 0.1 mM), aliquoted and stored at -80 °C. Viral stock titers were determined on Vero
301 E6 cells by plaque-forming assay and were expressed as plaque-forming units (PFU)
302 per ml. Virus stocks were also determined by flow cytometry as described ⁵⁴. Vero E6
303 cells were incubated 1 hour with 100 µl of tenfold serial dilutions of viral stocks. The
304 inoculum was then replaced with 500 µl of culture medium and the percentage of
305 infected cells was quantified by flow cytometry using the 2H2 anti-PrM mAb at 8 h after
306 infection. Viral titers were calculated and expressed as FIU per ml: Titer = (average
307 percentage of infection) x (number of cells in well) x (dilution factor) / (ml of inoculum
308 added to cells).

309 To establish a DENV replicon plasmid, based on the infectious DENV2-
310 16681 cDNA clone, the region encoding the structural proteins was mostly deleted and
311 replaced by a cassette encoding ubiquitin - Renilla luciferase - foot-and-mouth disease
312 virus (FMDV) 2A. DENV replicon RNA was generated as previously described ¹¹.
313 Infection or replication was determined by measuring the luciferase activity using
314 TriStar LB942 microplate reader (Berthold Technologies). RFP-expressing lentiviral
315 vector pseudotyped with vesicular stomatitis virus glycoprotein G (VSV-G) were
316 generated by transfecting HEK293FT cells with pNL4.3 Luc RFP ΔEnv, psPAX2 and
317 pVSV-G (4:3:1 ratio) using lipofectamine 3000. Supernatants were harvested 48 h after
318 transfection, cleared by centrifugation, filtered, and frozen at -80°C.

319 **Antibodies and reagents.**

320 All antibodies and reagents are listed in Table 3

321 **Polysome profiling.**

322 2×10^8 of indicated cells were incubated with 100 $\mu\text{g}/\text{mL}$ of cycloheximide (CHX) for
323 10 min at 37°C and washed twice with cold PBS + 100 $\mu\text{g}/\text{mL}$ CHX. Cells were pelleted
324 by centrifugation at 4°C , $300 \times g$ for 10 min and washed once with cold PBS + 100
325 $\mu\text{g}/\text{mL}$ CHX. The pellet was resuspended in 2 ml Lysis Buffer (10 mM Tris-HCl pH7.5;
326 100 mM KCl; 10 mM Magnesium acetate; 1% Triton X100; 2 mM DTT) containing 100
327 $\mu\text{g}/\text{ml}$ CHX. Cells were pulverized by adding glass beads and vortexed for 5 min at
328 4°C . Cells debris were removed by centrifugation at 4°C , $3,000 \times \text{rpm}$ for 10 min and
329 the supernatant was transferred to a 2 ml cryovial. The determination of polysome
330 concentration was done by spectrophotometric estimation, based on the fact that
331 ribosomes are ribonucleoprotein particles. Supernatant was quickly flash-frozen in
332 liquid nitrogen and stored in a -80°C freezer. The supernatant was loaded on a 10–
333 50 % sucrose gradient (31% sucrose; 50 mM Tris-acetate pH 7.6; 50 mM NH_4Cl ; 12
334 mM MgCl_2 ; 1 mM DTT) and spinned for 3 h at 39,000 rpm, 4°C , in an SW41 swing-
335 out rotor. The gradient was fractionated by hand and analyzed by immunoblotting.

336 **Mass spectrometry analysis.**

337 HAP1 cells (5×10^8), expressing either the WT or the HA-tagged RACK1 proteins,
338 were lysed in Pierce IP lysis buffer (Thermo Scientific) in the presence of Halt protease
339 inhibitor cocktail (Thermo Scientific) for 30 min at 4°C and then cleared by
340 centrifugation for 30 min at $6,000 \times g$. Supernatants were incubated overnight at 4°C
341 with anti-HA magnetic beads. Beads were washed three times with B015 buffer (20
342 mM Tris-HCl pH 7.4, 150 mM NaCl, 5 mM MgCl_2 , 10% glycerol, 0.5 mM EDTA, 0.05%
343 Triton, 0.1% Tween-20) and immune complexes were eluted twice with HA peptide
344 (400 mg/mL) 30 min at room temperature (RT). Eluates were concentrated on a Pierce
345 Concentrator, PES 10K, and stored at -20°C until used. A total of three co-affinity
346 purifications and MS analysis experiments were performed with the HA-tagged RACK1

347 protein or the untagged RACK1 protein as a control in 293T cells. Samples were
348 analyzed at Taplin Biological Mass Spectrometry Facility (Harvard Medical School).
349 Briefly, concentrated eluates issued from immunopurification of endogenous and
350 RACK1-HA-tagged protein are separated on 10% Tris-glycine SDS-PAGE gels
351 (Invitrogen), and stained with Imperial Protein Stain (Thermo Fisher). Individual regions
352 of the gel were cut into 1 mm³ pieces and subjected to a modified in-gel trypsin
353 digestion procedure⁵⁵. Peptides were desalted and subjected to a nano-scale reverse-
354 phase HPLC⁵⁶. Eluted peptides were then subjected to electrospray ionization and
355 then MS/MS analysis into an LTQ Orbitrap Velos Pro ion-trap mass spectrometer
356 (Thermo Fisher Scientific, Waltham, MA). Peptides were detected, isolated, and
357 fragmented to produce a tandem mass spectrum of specific fragment ions for each
358 peptide. Peptide sequences were determined by matching protein databases with the
359 acquired fragmentation pattern by the Sequest software program (Thermo Fisher
360 Scientific, Waltham, MA)⁵⁷. All databases include a reversed version of all the
361 sequences, and the data were filtered to < 2% peptide false discovery rate.

362 **Network analysis.**

363 The AP-MS dataset was analyzed with SAINTexpress and MIST software³⁷. Of the
364 1671 proteins selected in our pipeline, 193/1671 showed a probability score > 0.80
365 with SAINTexpress and 135/193 showed an AveragePeptide Count > 10. This list of
366 135 host proteins was analyzed with DAVID 6.8 to identify statistical enrichments for
367 specific GO terms from the “cellular component” (CC) annotation^{38,39}. The interaction
368 network was built using Cytoscape 3.4.0⁴⁰, and proteins were clustered into functional
369 modules using enriched GO terms as a guideline and manual curation of literature.

370 **siRNA Screen Assay**

371 An arrayed ON-TARGETplus SMARTpool siRNA library targeting 49/135 proteins of
372 our RACK1 network, which had an average peptide count > 28 was purchased from
373 Horizon Discovery. To this end, HeLa or 293T cells were transfected with a 30 nM final
374 concentration of siRNA using the Lipofectamine RNAiMax (Life Technologies). 48 hrs
375 post-transfection, cells were infected with DENV2-16681 at MOI 5. Infection was
376 quantified 48 hrs post infection by flow cytometry and viability by CellTiter-Glo 2.0
377 Assay (Promega). Two siRNA controls were included in the screen: a non-targeting
378 siRNA used as a reference (siNT) and a siRNA targeting RACK1 (siRACK1) as a
379 positive control for host dependency factors (HDFs)¹². HDFs were defined as factors
380 whose inhibition in both cell types decreases infection by at least 50% compared to
381 siNT and viability by at most 20% of the siNT.

382 **Gene editing and *trans*-complementation experiments.**

383 sgRNA targeting Vigilin, SERBP1 and ZNF598 were designed using the CRISPOR
384 software⁵⁸. Sequences for all the sgRNAs are listed in the Table 1. The sgRNAs were
385 cloned into the plasmid lentiCRISPR v2 (Addgene) according to the recommendations
386 provided by the members of the Zhang's laboratory (Broad Institute, Cambridge, MA .
387 HAP1 cells were transiently transfected with the plasmid expressing sgRNAs and
388 selected with puromycin until all mock-transfected cells died. Clonal cell lines were
389 isolated by limiting dilution and assessed by DNA sequencing and immunoblot for gene
390 editing. The human HA-RACK1 WT and HA-RACK1 DE mutant plasmid were provided
391 by the Gabriele Fuchs Lab (University at Albany) , the FLAG-tagged Vigilin cDNA was
392 purchased from Genscript (Clone ID: OHu17734) and the Myc-tagged SERBP1 cDNA
393 was purchased from Genscript (Clone ID: OHu26811C). After PCR, amplification
394 products were cloned into a SpeI-NotI (RACK1), NotI-XhoI (Vigilin) or EcoRI-BamHI
395 (SERBP1) digested pLVX-IRES-ZsGreen1 vector. SERBP1 mutant and Vigilin mutant

396 were obtained using the Q5® Site-Directed Mutagenesis Kit (E0554) (NEB) with
397 deletion primers using the WT cDNA in pLVX as template. All primers are listed in
398 Table 1. Lentiviral like particles for transduction were prepared in 293T cells by co-
399 transfecting the plasmid of interest with psPAX2 (from N. Manel's lab, Curie Institute,
400 Paris) and pCMV-VSV-G at a ratio of 4:3:1 with Lipofectamine 3,000 (Thermo Fisher
401 Scientific). Supernatants were collected 48 h after transfection, centrifugated (750 g,
402 10 min), filtered using a 0.45µm filter, and purified through a 20% sucrose cushion by
403 ultracentrifugation (80,000 g for 2 h at 4°C). Pellets were resuspended in HNE1X pH
404 7.4, aliquoted, and stored at -80°C. Cells of interest were transduced by spinoculation
405 (750 g for 2 h at 32°C) and sorted for GFP-positive cells by flow cytometry if necessary.

406 **Flow cytometry analysis.**

407 Indicated cells were plated in 24 well plates and infected. At indicated times, cells were
408 trypsinized and fixed with 2% paraformaldehyde (PFA) diluted in PBS for 15 min at
409 room temperature. Cells were incubated for 1 hour at 4°C with 1 µg/ml of 3E4 anti-E2
410 monoclonal antibody (CHIKV), 2H2 anti-prM monoclonal antibody (mAb) (DENV) or
411 the anti-E protein mAb 4G2 (ZIKV). Antibodies were diluted in permeabilization flow
412 cytometry buffer (PBS supplemented with 5% FBS, 0.5% saponin, 0.1% sodium
413 azide). After washing, cells were incubated with 1 µg/ml of Alexa Fluor 488 or 647-
414 conjugated goat anti-mouse IgG diluted in permeabilization flow cytometry buffer for
415 30 min at 4°C. Acquisition was performed on Attune NxT Flow Cytometer (Thermo
416 Fisher Scientific) and data were analyzed by FlowJo software (TreeStar).

417 **Infectious virus yield assay.**

418 To assess the release of infectious particles during infection, indicated cells were
419 inoculated for 3 h with DENV2-16681, washed once with PBS and maintained in the
420 culture medium for 48 h. At the indicated time points, supernatants were collected and

421 kept at -80°C. Vero E6 cells were incubated with three-fold serial dilutions of
422 supernatant for 24 h and prM expression was quantified by flow cytometry as
423 previously described ⁵⁴.

424 **Immunoblots.**

425 Cell pellets were lysed in Pierce IP Lysis Buffer (Thermo Fisher Scientific) containing
426 Halt protease and phosphatase inhibitor cocktails (Thermo Fisher Scientific) for 30 min
427 at 4 °C. Equal amounts of protein, determined by DC Protein Assay (BioRad), were
428 prepared in 4X LDS sample buffer (Pierce) containing 25 mM dithiothreitol (DTT) and
429 heated at 95 °C for 5 min. Samples were separated on Bolt 4–12% Bis-Tris gels in Bolt
430 MOPS SDS Running Buffer (Thermo Scientific) and proteins were transferred onto a
431 PVDF membrane (BioRad) using the Power Blotter system (Thermo Fisher Scientific).
432 Membranes were blocked with PBS containing 0.1% Tween-20 and 5% non-fat dry
433 milk and incubated overnight at 4 °C with primary antibodies (HA 1/5,000, RACK1
434 1/4,000, GAPDH 1/5,000, Vigilin 1/500, SERBP1 1/2,000, NS3 DENV 1/4,000, 2H2
435 prM DENV 1/4,000, E DENV 1/5,000, FLAG 1/2,000, Myc 1/1,000, Tubulin 1/500,
436 ZNF598 1/10,000, Anti Mouse HRP 1/5,000, Anti Rabbit HRP 1/10,000 . Staining was
437 revealed with corresponding horseradish peroxidase (HRP)-coupled secondary
438 antibodies and developed using Super Signal West Dura Extended Duration Substrate
439 (Thermo Fisher Scientific) following the manufacturer's instructions. The signals were
440 acquired with Fusion Fx camera (VILBERT Lourmat).

441 **Co-immunoprecipitation assay.**

442 Indicated cells were plated in 10 cm dishes (5×10^6) After 24 h, the cells were
443 transfected with a total of 15 µg DNA expression plasmids (7.5 µg of each plasmid in
444 co-transfection assays) using Lipofectamine 3,000 (Thermo Fisher Scientific). After 24
445 h of transfection, the cells were washed once with PBS, collected, and centrifugated

446 (400g for 5 min). Cell pellets were lysed in Pierce IP Lysis Buffer (Thermo Fisher
447 Scientific) containing Halt protease and phosphatase inhibitor cocktails (Thermo Fisher
448 Scientific) for 30 min at 4 °C. Equal amounts of protein, determined by DC Protein
449 Assay (BioRad), were incubated overnight at 4 °C, with either anti-FLAG magnetic
450 beads, anti-HA magnetic beads or anti-Myc magnetic beads. Beads were washed
451 three times with BO15 buffer (20 mM Tris-HCl pH 7.4, 150 mM NaCl, 5 mM MgCl₂,
452 10% glycerol, 0.5 mM EDTA, 0.05% Triton X-100, 0.1% Tween-20) before incubation.
453 The retained complexes were eluted twice with either 3x FLAG peptide (200 µg/ml
454 Sigma-Aldrich), HA peptide (400 µg/ml Roche) or cMyc peptide (200 µg/ml Sigma-
455 Aldrich) for 30 min at RT. Samples were prepared and immunoblotted as described
456 above. For input, 1% of whole-cell lysates was loaded on the gel.

457 **RNA preparation and quantitative RT-qPCR.**

458 Total RNA extraction from the indicated cells was performed using the RNeasy Plus
459 Mini kit (Qiagen). RNA was quantified using a Nanodrop One (Thermo Fisher
460 Scientific) before cDNA amplification. cDNA was prepared from 100 ng total RNA with
461 Maxima First Strand Synthesis Kit (Thermo Fisher Scientific) including an additional
462 step of RNase H treatment after reverse transcription. RT-qPCR was performed using
463 Power Syber green PCR master Mix (Thermo Fisher Scientific) on a Light Cycler 480
464 (Roche). Quantification was based on the comparative threshold cycle (Ct) method,
465 using GAPDH as endogenous reference control. All primers are listed in Table 1.

466 **RNA immunoprecipitation (RNA-IP).**

467 Indicated cells (2×10^6) were plated in 10 cm dishes, transfected 48 h with the
468 corresponding plasmids using Lipofectamine 3000 and then infected with DENV2-
469 16681 at m.o.i 2. 48 h post infection, culture media was removed, and cells were
470 washed twice with cold PBS. 10 ml of cold PBS were added on the cell before UV

471 cross-link (2000mJ/cm²). Cells were collected and spun 5 min at 4°C 2,000 rpm. Cell
472 pellets were lysed in 1 ml of Pierce IP Lysis Buffer (Thermo Fisher Scientific) containing
473 Halt protease and phosphatase inhibitor cocktails (Thermo Fisher Scientific) + 250 U
474 of RNasin (Promega) for 30 min at 4 °C. 250 U of turbo DNase was added and the
475 lysate was put 30 min at 37°C and centrifugated at 15,000 rpm for 15 min. The
476 supernatant was then collected. The protein of interest was immunoprecipitated and
477 eluted (see co-immunoprecipitation assay). 100 µl of Input and Elution were incubated
478 with 150 µl of proteinase K buffer (117 µl NT-2, 15 µl SDS 10 %, and 18 µl of Proteinase
479 K) 1 h at 56°C and then 750 µl of Trizol Reagent was added. RNA was extracted by
480 phenol chloroform precipitation: 0.2 ml of chloroform per 1 ml of TRIZOL Reagent was
481 added. Samples were vortexed vigorously for 15 seconds and incubated at room
482 temperature for 2 to 3 minutes and then centrifuged at 12,000 x g for 15 minutes at
483 4°C. Following centrifugation, the upper aqueous phase was transferred carefully
484 without disturbing the interphase into fresh tube. The RNA from the aqueous phase
485 was precipitated by mixing with 0.5 ml of isopropyl alcohol per 1 ml of TRIZOL reagent
486 used for the initial homogenization. Samples was incubated at RT for 10 minutes and
487 centrifuged at 12,000 x g for 10 minutes at 2 to 4°C. The supernatant was removed
488 completely, and the RNA pellet was washed twice with 1 ml of 75% ethanol per 1 ml
489 of TRIZOL Reagent used for the initial homogenization. The samples were mixed by
490 vortexing and centrifuged at 7,500 x g for 5 minutes at 2 to 8°C. The RNA pellet was
491 air dried for 5-10 minutes and then dissolved in RNase free water.

492 **Cell viability assay.**

493 Cell viability and proliferation were assessed using CellTiter-Glo 2.0 assay (Promega)
494 according to the manufacturer's protocol. Cells (3×10^4) were plated in 48 well plates.
495 At the indicated times, 100 µl of CellTiter-Glo reagent were added to each well. After

496 10 min of incubation, 200 μ l from each well was transferred in an opaque 96-well plate
497 (Cellstar, Greiner Bio-One) and luminescence was measured on a TriStar2 LB 942
498 (Berthold) with 0.1 s integration time.

499 **RNA stability measurement by high molecular weight northern blot analysis.**

500 Indicated cells (1×10^6) were plated on a 60-mm dish and infected with DENV2-16681.
501 48 h post infection, medium was replaced by MK0608 (50 μ M final concentration)
502 containing medium to block viral replication. At the indicated time post treatment, cells
503 were washed twice with cold PBS and harvested in TRIzol (Thermo Fisher Scientific).
504 Total RNA extraction was performed as previously described in RIP protocol. The
505 DENV2-specific probe was obtained after PCR amplification of the 3'UTR of the
506 DENV2-16681 infectious clone (from 10,205 to 10,704). Probes were then labeled with
507 α - 32 P dCTP using the Prime-a-gene kit (Promega). For high molecular weight northern
508 blot analysis to detect DENV2 genomic RNA, 5 μ g of total RNA were denatured for 5
509 minutes at 65°C in RNA sample buffer (32% deionized formamide, 4% formaldehyde,
510 1X MOPS, ethidium bromide 1 μ g/ μ l). Then, RNA loading buffer (50% glycerol, EDTA
511 1mM, 0.4% bromophenol blue) was added. RNAs were resolved in a 1% agarose gel
512 containing 1X MOPS and 3.7% formaldehyde in 1X MOPS buffer, before being
513 transferred overnight on a nylon Hybond N+ membrane (Cytiva) in a 20X SSC solution
514 (Euromedex). RNAs were UV crosslinked (120 mJoules) with Stratagene Stratalinker
515 1800 (LabX). Membrane was blocked and hybridized overnight at 42°C using
516 PerfectHybTM Plus hybridization buffer (Sigma) with the corresponding labeled probe.
517 The day after, the membrane was washed using 2X SSC, 0.1% SDS solution twice at
518 42°C and 0.1X SSC, 0.1% SDS twice at 50°C before being exposed on an Image Plate
519 (Fujifilm) during 24 h. The plate was revealed using TyphoonTM FLA 7,000 (GE

520 Healthcare). Densitometry analysis of the bands was performed using Image Quant
521 TL 8.1 software (GE healthcare).

522 **Graphics and statistical analyses.**

523 The number of independent experimental replications is indicated in the legends.
524 Graphical representation and statistical analyses of mean and s.e.m. were performed
525 using Prism 8 software (GraphPad Software) as well as Student's t-test.

526

527

528 **Acknowledgements**

529 This study has received funding from the Fondation pour la Recherche Medicale (grant
530 FRM - EQU202003010193), the French Government's Investissement d'Avenir
531 program, Laboratoire d'Excellence "Integrative Biology of Emerging Infectious
532 Diseases" (grant n°ANR-10-LABX-62-IBEID), the ANR-15-CE15-00029 ZIKAHOST.
533 A.B was funded by a scholarship from the French Ministry of Research. The authors
534 thank Karim Majzoub, Alessia Zamborlini for critical readings of the manuscript and
535 helpful discussions. The authors are grateful to Ralf Bartenschlager (Heidelberg
536 University, Germany) and Dr Gabriele Fucks (University at Albany, NY, 12222, USA)
537 for providing us with DENV R2A reporter virus and RACK1 knockout cells and
538 plasmids, respectively. Ali Amara dedicates this work to the memory of Professor Jean-
539 Louis Virelizier (Unité d Immunologie Virale, Institut Pasteur, Paris) and Professor
540 Renaud Mahieux (Ecole Normale Supérieure, Lyon, France), who left us during the
541 SARS-CoV-2 epidemic.

542
543 **Author's contributions**

544 A.B., MLH, and A.A conceived the study. A.B., M.L.H., M.P, L.C., L.B.M., C.D., L.M.
545 and A.A. designed the experiments. A.B. and M.L.H. performed the RACK1
546 interactome and the RNAi screen. P.O.V. provided help in the data analysis. M.P.,
547 L.C., L.B.M., and V.K. generated the viruses used in this study and performed infection
548 studies. B.M.K. generated the DENV replicon and provided expertise in viral RNA
549 production. S.P. and M.B. performed the DENV RNA stability experiments. S.G.M.
550 participated in the RNA-IP experiments. A.B. and A.A. wrote the initial manuscript draft,
551 and the other authors contributed to its editing in its final form.

552
553 **Competing interest statement**

554 The authors declare no competing financial interests.

555

556

557 **Materials & Correspondence**

558 Correspondence and material requests should be addressed to Dr Ali Amara

559 (ali.amara@inserm.fr)

560

561 **Legends**

562
563 **Figure 1: The interaction between RACK1 and the 40S ribosome is required for**

564 **DENV infection**

565 **(a)** Western Blot analysis of RACK1 expression in control, RACK1^{KO} and RACK1^{KO}
566 HAP1 cells trans-complemented with a HA-RACK1 cDNA. Cell lysates were probed
567 with the indicated antibodies. Representative western blot of n=3 technically
568 independent experiments. **(b)** Role of RACK1 in DENV infection. Controls, RACK1^{KO}
569 or RACK1^{KO} cells transcomplemented with a cDNA encoding WT HA-RACK1 were
570 infected at different m.o.i with DENV2-16681. Levels of infection were determined by
571 flow cytometry using the 2H2 prM mAb at 48 hpi. Data shown are mean +/- s.e.m of 4
572 independent experiments performed in duplicate. Significance was calculated using
573 two-way ANOVA with Dunnett's multiple comparison test **(c)** Western Blot analysis of
574 RACK1 expression in RACK1^{KO} HAP1 transcomplemented with cDNA encoding WT
575 HA-RACK1 or the HA-RACK1 D/E mutant. Cells lysates were probed with the indicated
576 antibodies. Representative western blot of 3 independent experiments. **(d)** Impact of
577 RACK1 association to the 40S subunit of the ribosome in DENV infection. Control,
578 RACK1^{KO} and RACK1^{KO} HAP1 cells trans-complemented with cDNA encoding WT
579 HA-RACK1 or the HA-RACK1 DE mutant were infected at m.o.i 1 with DENV2-16681
580 and harvested at 48 hpi. Levels of infection were determined by flow cytometry as
581 described above. Data shown are mean +/- s.e.m of 3 independent experiments
582 performed in duplicate. Significance was calculated using one-way ANOVA with
583 Dunnett's multiple comparison test. ns, not significant; ****, $P < 0.0001$

584

585

586 **Figure 2: Global map of the RACK1 interactome in human cells**

587 **(a)** Experimental scheme of our RACK1 immunoprecipitation approach. 293T cells
588 expressing RACK1 or HA-RACK1 were lysed, and extracts were purified with anti-HA-
589 coated beads before SDS-PAGE and mass spectrometry (MS) analysis. **(b)** Histogram
590 indicating statistical enrichment for specific biological processes (BP) and cellular
591 components (CC), determined by Gene Ontology (GO) analysis. **(c)** Interaction
592 network of RACK1-associated proteins identified by MS in 293T cells. Proteins were
593 clustered into functional modules using enriched GO terms as a guideline and manual
594 mining of literature. Representative network of n=3 independent experiments showing
595 similar results.

596

597 **Figure 3: Vigilin, SERBP1 and ZNF598 are DENV host dependency factors**

598 **(a)** Host dependency factors (HDFs) found in our RNAi screen. Data shown are
599 representative of 3 independent experiments. Host dependency factors are marked in
600 green. Positive control (siRNA pool targeting RACK1) is highlighted in blue. **(b)**
601 Validation of the interaction between RACK1 and endogenous Vigilin or SERBP1 in
602 293T cells by immunoprecipitation. Cell extracts from 293T cells expressing RACK1 or
603 HA-RACK1 were subjected to affinity-purification using anti-HA beads and interacting
604 proteins were revealed by western blot. Data shown are representative of 3
605 independent experiments. **(c-e)** Impact of RACK1/Vigilin/SERBP1/ZNF598 gene
606 editing on DENV infectious cycle in HAP1 cells. The indicated cells were infected for
607 48 hrs at m.o.i 1 with DENV2-16681. **(c)** Supernatants from infected cells were
608 harvested, then titered by flow cytometry on Vero cells and expressed as FIU/ml. FIU,
609 FACS Infectious Unit. **(d)** Infection was assessed by immunoblot using anti-NS3, anti-
610 prM and anti-E DENV mAb. Data shown are representative of 3 independent
611 experiments. **(e)** Levels of infection were assessed by quantification of DENV vRNA

612 by qRT-PCR using NS3 primers. **(c and d)** Data shown are mean +/- s.e.m of 3
613 independent experiments performed in duplicate. Significance was calculated using a
614 two-tailed Student's t test. **(f)** The indicated cells were infected with ZIKV HD78 at
615 m.o.i 2 (left), CHIKV 21 at m.o.i 2 (middle), VSV-pp at m.o.i 2 (right). Levels of infection
616 were determined by flow cytometry at 48 hpi. Data shown are mean +/- s.e.m of at
617 least 2 independent experiments performed in duplicate. Significance was calculated
618 using one-way ANOVA with Dunnett's multiple comparison test.. ns: not significant;
619 ****: $P < 0.0001$

620

621 **Figure 4: Vigilin and SERBP1 regulate DENV translation and replication**

622 **(a)** The indicated cells were infected at m.o.i 1 with DENV-Luc. At indicated time points
623 Renilla luciferase activity reflecting RNA translation (1 to 8 hpi) and replication (12 to
624 72 hpi) was measured. Data shown are mean +/- s.e.m of 3 independent experiments
625 performed in triplicate. two-way ANOVA with Dunnett's multiple comparison test. **(b)**
626 Indicated cells were infected at m.o.i 1 with CHIKV-Luc. Gaussia luciferase activity was
627 monitored at the indicated time points. Data shown are mean +/- s.e.m of 3
628 independent experiments performed in triplicate. Significance was calculated using
629 two-way ANOVA with Dunnett's multiple comparison test. **(c)** Impact of
630 RACK1/Vigilin/SERBP1 KO on DENV life cycle in HAP1 cells transfected with a DENV
631 replicon RNA expressing Renilla luciferase. Renilla luciferase activity was monitored
632 at the indicated time point. Data shown are mean +/- s.e.m of 3 independent
633 experiments performed in triplicate. Significance was calculated using two-way
634 ANOVA with Dunnett's multiple comparison test. ns: not significant; ****: $P < 0.0001$.

635 **Figure 5: Vigilin and SERBP1 interaction with RACK1 is important for DENV** 636 **infection**

637 **(a)** Evaluation of FLAG-Vigilin mutant (left) or Myc-SERBP1 mutant (right) interaction
638 with RACK1. Cell extracts from 293T expressing Wt or mutated form of Vigilin and
639 SERBP1 were subjected to affinity-purification using anti-FLAG or -Myc coated beads,
640 respectively. Input and eluates were resolved by SDS-PAGE and interacting proteins
641 were revealed by western blot using corresponding antibodies. Representative
642 western blot of 3 independent experiments. **(b)** RIP analysis of the interaction of Vigilin
643 (WT and Mut) and SERBP1 (WT and Mut) with the DENV vRNA. Cells were infected
644 at m.o.i 1 by DENV2-16681 and harvested 48 hpi. Tagged-proteins were
645 immunoprecipitated after UV crosslink at 254 nm using anti-FLAG or -Myc coated
646 beads. The amount of vRNA in the input (in purple) and the elution fractions (in orange)
647 were determined by RT-qPCR using DENV2 specific primers. Data shown are mean
648 +/- s.e.m of 3 independent experiments performed in triplicate. Significance was
649 calculated using a one-way ANOVA with Dunnett's multiple comparison test **(c)** DENV
650 infection in HAP1 cells expressing Vigilin (WT or Mut) and SERBP1 (WT or Mut). The
651 indicated cells were infected at m.o.i 1 with DENV2-16681 . Levels of infection were
652 determined by flow cytometry at 48 hpi. Data shown are mean +/- s.e.m of 3 technically
653 independent experiments performed in duplicate. . Significance was calculated using
654 one-way ANOVA with Dunnett's multiple comparison test. ns: not significant; ****: $P <$
655 0.0001.

656
657

658

659

660

661

662 References:

- 663 1. Holbrook, M. R. Historical Perspectives on Flavivirus Research. *Viruses* **9**, 97 (2017).
664 2. Halstead, S. B. Dengue. *Lancet Lond. Engl.* **370**, 1644–1652 (2007).
665 3. Brady, O. J. *et al.* Refining the global spatial limits of dengue virus transmission by
666 evidence-based consensus. *PLoS Negl. Trop. Dis.* **6**, e1760 (2012).
667 4. Bhatt, S. *et al.* The global distribution and burden of dengue. *Nature* **496**, 504–507
668 (2013).
669 5. Kaptein, S. J. F. *et al.* A pan-serotype dengue virus inhibitor targeting the NS3-
670 NS4B interaction. *Nature* **598**, 504–509 (2021).
671 6. Hadinegoro, S. R. *et al.* Efficacy and Long-Term Safety of a Dengue Vaccine in
672 Regions of Endemic Disease.
673 <http://dx.doi.org.proxy.insermbiblio.inist.fr/10.1056/NEJMoa1506223> <https://www.nejm->
674 [org.proxy.insermbiblio.inist.fr/doi/10.1056/NEJMoa1506223](http://www.nejm.org.proxy.insermbiblio.inist.fr/doi/10.1056/NEJMoa1506223) (2015)
675 doi:10.1056/NEJMoa1506223.
676 7. Ferguson, N. M. *et al.* Benefits and risks of the Sanofi-Pasteur dengue vaccine:
677 Modeling optimal deployment. *Science* **353**, 1033–1036 (2016).
678 8. Acosta, E. G., Kumar, A. & Bartenschlager, R. Revisiting dengue virus-host cell
679 interaction: new insights into molecular and cellular virology. *Adv. Virus Res.* **88**, 1–109
680 (2014).
681 9. Zeidler, J. D., Fernandes-Siqueira, L. O., Barbosa, G. M. & Da Poian, A. T. Non-
682 Canonical Roles of Dengue Virus Non-Structural Proteins. *Viruses* **9**, 42 (2017).
683 10. Miller, S. & Krijnse-Locker, J. Modification of intracellular membrane structures for
684 virus replication. *Nat. Rev. Microbiol.* **6**, 363–374 (2008).
685 11. Welsch, S. *et al.* Composition and Three-Dimensional Architecture of the Dengue
686 Virus Replication and Assembly Sites. *Cell Host Microbe* **5**, 365–375 (2009).
687 12. Hafirassou, M. L. *et al.* A Global Interactome Map of the Dengue Virus NS1 Identifies
688 Virus Restriction and Dependency Host Factors. *Cell Rep.* **21**, 3900–3913 (2017).
689 13. Shue, B. *et al.* Genome-wide CRISPR screen identifies RACK1 as a critical host
690 factor for flavivirus replication. *J. Virol.* JVI0059621 (2021) doi:10.1128/JVI.00596-21.
691 14. Ben-Shem, A. *et al.* The Structure of the Eukaryotic Ribosome at 3.0 Å Resolution.
692 *Science* **334**, 1524–1529 (2011).
693 15. Sengupta, J. *et al.* Identification of the versatile scaffold protein RACK1 on the
694 eukaryotic ribosome by cryo-EM. *Nat. Struct. Mol. Biol.* **11**, 957–962 (2004).
695 16. Xu, C. & Min, J. Structure and function of WD40 domain proteins. *Protein Cell* **2**,
696 202–214 (2011).
697 17. Nielsen, M. H., Flygaard, R. K. & Jenner, L. B. Structural analysis of ribosomal
698 RACK1 and its role in translational control. *Cell. Signal.* **35**, 272–281 (2017).
699 18. Adams, D. R., Ron, D. & Kiely, P. A. RACK1, A multifaceted scaffolding protein:
700 Structure and function. *Cell Commun. Signal. CCS* **9**, 22 (2011).
701 19. Gandin, V., Senft, D., Topisirovic, I. & Ronai, Z. A. RACK1 Function in Cell Motility
702 and Protein Synthesis. *Genes Cancer* **4**, 369–377 (2013).
703 20. Chang, B. Y., Conroy, K. B., Machleder, E. M. & Cartwright, C. A. RACK1, a
704 Receptor for Activated C Kinase and a Homolog of the β Subunit of G Proteins, Inhibits
705 Activity of Src Tyrosine Kinases and Growth of NIH 3T3 Cells. *Mol. Cell. Biol.* **18**, 3245–
706 3256 (1998).
707 21. Chang, B. Y., Harte, R. A. & Cartwright, C. A. RACK1: a novel substrate for the Src
708 protein-tyrosine kinase. *Oncogene* **21**, 7619–7629 (2002).
709 22. Yarwood, S. J., Steele, M. R., Scotland, G., Houslay, M. D. & Bolger, G. B. The
710 RACK1 Signaling Scaffold Protein Selectively Interacts with the cAMP-specific

- 711 Phosphodiesterase PDE4D5 Isoform. *J. Biol. Chem.* **274**, 14909–14917 (1999).
- 712 23. Kiely, P. A., Sant, A. & O'Connor, R. RACK1 Is an Insulin-like Growth Factor 1
713 (IGF-1) Receptor-interacting Protein That Can Regulate IGF-1-mediated Akt Activation and
714 Protection from Cell Death. *J. Biol. Chem.* **277**, 22581–22589 (2002).
- 715 24. Baum, S., Bittins, M., Frey, S. & Sedorf, M. Asc1p, a WD40-domain containing
716 adaptor protein, is required for the interaction of the RNA-binding protein Scp160p with
717 polysomes. *Biochem. J.* **380**, 823–830 (2004).
- 718 25. Ceci, M. *et al.* Release of eIF6 (p27BBP) from the 60S subunit allows 80S ribosome
719 assembly. *Nature* **426**, 579–584 (2003).
- 720 26. Joshi, B. *et al.* Phosphorylation of Eukaryotic Protein Synthesis Initiation Factor 4E at
721 Ser-209 *. *J. Biol. Chem.* **270**, 14597–14603 (1995).
- 722 27. Whalen, S. G. *et al.* Phosphorylation of eIF-4E on Serine 209 by Protein Kinase C Is
723 Inhibited by the Translational Repressors, 4E-binding Proteins (*). *J. Biol. Chem.* **271**,
724 11831–11837 (1996).
- 725 28. Sundaramoorthy, E. *et al.* ZNF598 and RACK1 Regulate Mammalian Ribosome-
726 Associated Quality Control Function by Mediating Regulatory 40S Ribosomal Ubiquitylation.
727 *Mol. Cell* **65**, 751-760.e4 (2017).
- 728 29. Long, L. *et al.* Recruitment of Phosphatase PP2A by RACK1 Adaptor Protein
729 Deactivates Transcription Factor IRF3 and Limits Type I Interferon Signaling. *Immunity* **40**,
730 515–529 (2014).
- 731 30. Xie, T. *et al.* RACK1 attenuates RLR antiviral signaling by targeting VISA-TRAF
732 complexes. *Biochem. Biophys. Res. Commun.* **508**, 667–674 (2019).
- 733 31. Duan, Y. *et al.* RACK1 Mediates NLRP3 Inflammasome Activation by Promoting
734 NLRP3 Active Conformation and Inflammasome Assembly. *Cell Rep.* **33**, 108405 (2020).
- 735 32. Kuhn, L. *et al.* Definition of a RACK1 Interaction Network in *Drosophila*
736 *melanogaster* Using SWATH-MS. *G3 Bethesda Md* **7**, 2249–2258 (2017).
- 737 33. Majzoub, K. *et al.* RACK1 Controls IRES-Mediated Translation of Viruses. *Cell* **159**,
738 1086–1095 (2014).
- 739 34. Jha, S. *et al.* Trans-kingdom mimicry underlies ribosome customization by a poxvirus
740 kinase. *Nature* **546**, 651–655 (2017).
- 741 35. Kim, H. D., Kong, E., Kim, Y., Chang, J.-S. & Kim, J. RACK1 depletion in the
742 ribosome induces selective translation for non-canonical autophagy. *Cell Death Dis.* **8**, e2800
743 (2017).
- 744 36. Gallo, S. *et al.* RACK1 Specifically Regulates Translation through Its Binding to
745 Ribosomes. *Mol. Cell. Biol.* **38**, (2018).
- 746 37. Teo, G. *et al.* SAINTexpress: improvements and additional features in Significance
747 Analysis of Interactome software. *J. Proteomics* **100**, 37–43 (2014).
- 748 38. Huang, D. W., Sherman, B. T. & Lempicki, R. A. Systematic and integrative analysis
749 of large gene lists using DAVID bioinformatics resources. *Nat. Protoc.* **4**, 44–57 (2009).
- 750 39. Huang, D. W., Sherman, B. T. & Lempicki, R. A. Bioinformatics enrichment tools:
751 paths toward the comprehensive functional analysis of large gene lists. *Nucleic Acids Res.* **37**,
752 1–13 (2009).
- 753 40. Shannon, P. *et al.* Cytoscape: A Software Environment for Integrated Models of
754 Biomolecular Interaction Networks. *Genome Res.* **13**, 2498–2504 (2003).
- 755 41. Liu, Y. & Shi, S.-L. The roles of hnRNP A2/B1 in RNA biology and disease. *Wiley*
756 *Interdiscip. Rev. RNA* **12**, e1612 (2021).
- 757 42. Ahn, J.-W. *et al.* SERBP1 affects homologous recombination-mediated DNA repair
758 by regulation of CtIP translation during S phase. *Nucleic Acids Res.* **43**, 6321–6333 (2015).
- 759 43. Cheng, M. H. & Jansen, R.-P. A jack of all trades: the RNA-binding protein vigilin.
760 *Wiley Interdiscip. Rev. RNA* **8**, (2017).

- 761 44. Paranjape, S. M. & Harris, E. Y Box-binding Protein-1 Binds to the Dengue Virus 3'-
762 Untranslated Region and Mediates Antiviral Effects. *J. Biol. Chem.* **282**, 30497–30508
763 (2007).
- 764 45. Brunetti, J. E., Scolaro, L. A. & Castilla, V. The heterogeneous nuclear
765 ribonucleoprotein K (hnRNP K) is a host factor required for dengue virus and Junín virus
766 multiplication. *Virus Res.* **203**, 84–91 (2015).
- 767 46. Mobin, M. B. *et al.* The RNA-binding protein vigilin regulates VLDL secretion
768 through modulation of Apob mRNA translation. *Nat. Commun.* **7**, 12848 (2016).
- 769 47. Ooi, Y. S. *et al.* An RNA-centric dissection of host complexes controlling flavivirus
770 infection. *Nat. Microbiol.* **4**, 2369–2382 (2019).
- 771 48. Bolger, G. B. The RNA-binding protein SERBP1 interacts selectively with the
772 signaling protein RACK1. *Cell. Signal.* **35**, 256–263 (2017).
- 773 49. Brown, A., Baird, M. R., Yip, M. C., Murray, J. & Shao, S. Structures of
774 translationally inactive mammalian ribosomes. *eLife* **7**, e40486 (2018).
- 775 50. Phillips, S. L., Soderblom, E. J., Bradrick, S. S. & Garcia-Blanco, M. A. Identification
776 of Proteins Bound to Dengue Viral RNA In Vivo Reveals New Host Proteins Important for
777 Virus Replication. *mBio* **7**, (2016).
- 778 51. Wang, G., Kouwaki, T., Okamoto, M. & Oshiumi, H. Attenuation of the Innate
779 Immune Response against Viral Infection Due to ZNF598-Promoted Binding of FAT10 to
780 RIG-I. *Cell Rep.* **28**, 1961-1970.e4 (2019).
- 781 52. Li, A. *et al.* Both KH and non-KH domain sequences are required for polyribosome
782 association of Scp160p in yeast. *Nucleic Acids Res.* **32**, 4768–4775 (2004).
- 783 53. Meertens, L. *et al.* FHL1 is a major host factor for chikungunya virus infection.
784 *Nature* **574**, 259–263 (2019).
- 785 54. Meertens, L. *et al.* The TIM and TAM Families of Phosphatidylserine Receptors
786 Mediate Dengue Virus Entry. *Cell Host Microbe* **12**, 544–557 (2012).
- 787 55. Shevchenko, A., Wilm, M., Vorm, O. & Mann, M. Mass spectrometric sequencing of
788 proteins silver-stained polyacrylamide gels. *Anal. Chem.* **68**, 850–858 (1996).
- 789 56. J, P. & Sp, G. Proteomics: the move to mixtures. *Journal of mass spectrometry : JMS*
790 vol. 36 <https://pubmed-ncbi-nlm-nih-gov.proxy.insermbiblio.inist.fr/11747101/> (2001).
- 791 57. Eng, J. K., McCormack, A. L. & Yates, J. R. An approach to correlate tandem mass
792 spectral data of peptides with amino acid sequences in a protein database. *J. Am. Soc. Mass*
793 *Spectrom.* **5**, 976–989 (1994).
- 794 58. Concordet, J.-P. & Haeussler, M. CRISPOR: intuitive guide selection for
795 CRISPR/Cas9 genome editing experiments and screens. *Nucleic Acids Res.* **46**, W242–W245
796 (2018).
- 797
- 798

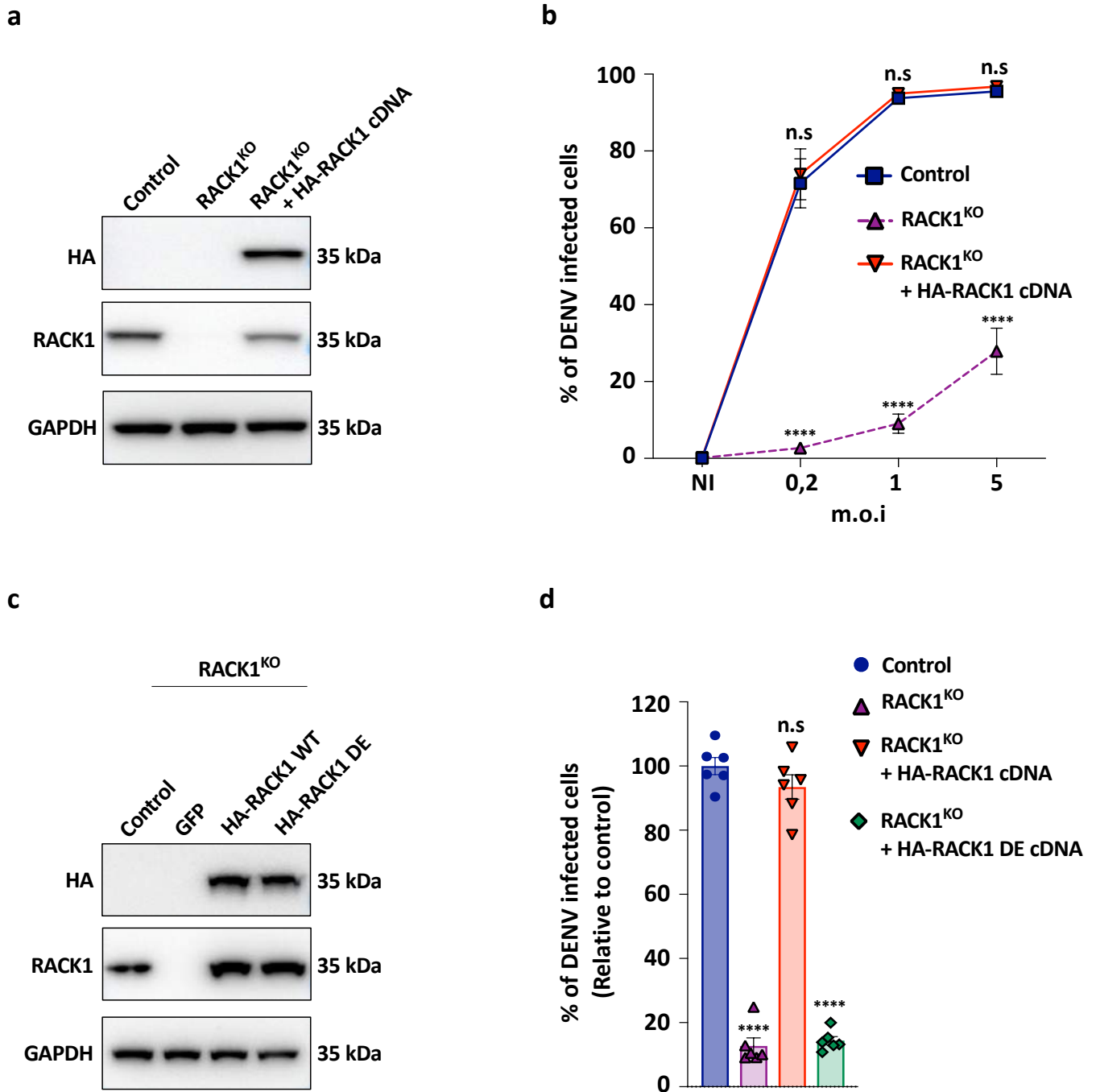


Figure 1

a

293T + / - HA-RACK1

Cell lysis

Input

HA IP

HA peptide elution

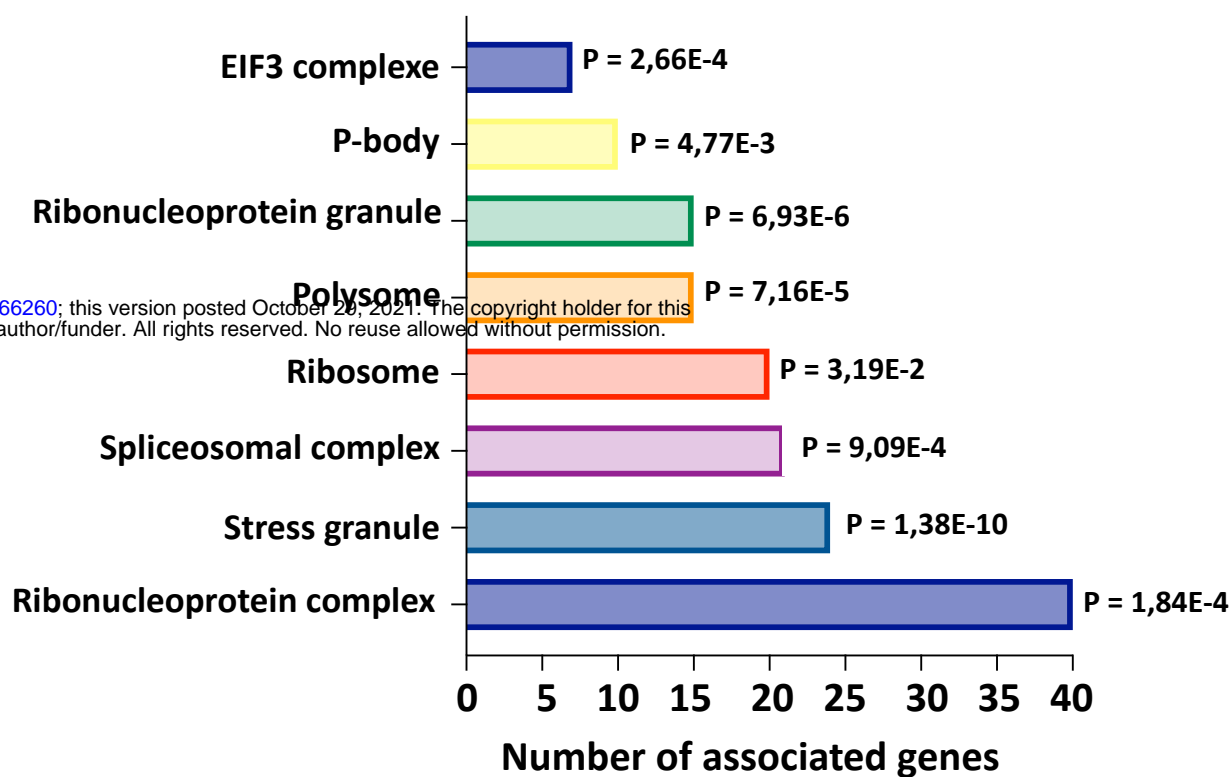
SDS Page

Silver Staining

LC-MS/MS

bioRxiv preprint doi: <https://doi.org/10.1101/2021.10.28.466260>; this version posted October 29, 2021. The copyright holder for this preprint (which was not certified by peer review) is the author/funder. All rights reserved. No reuse allowed without permission.

b



c

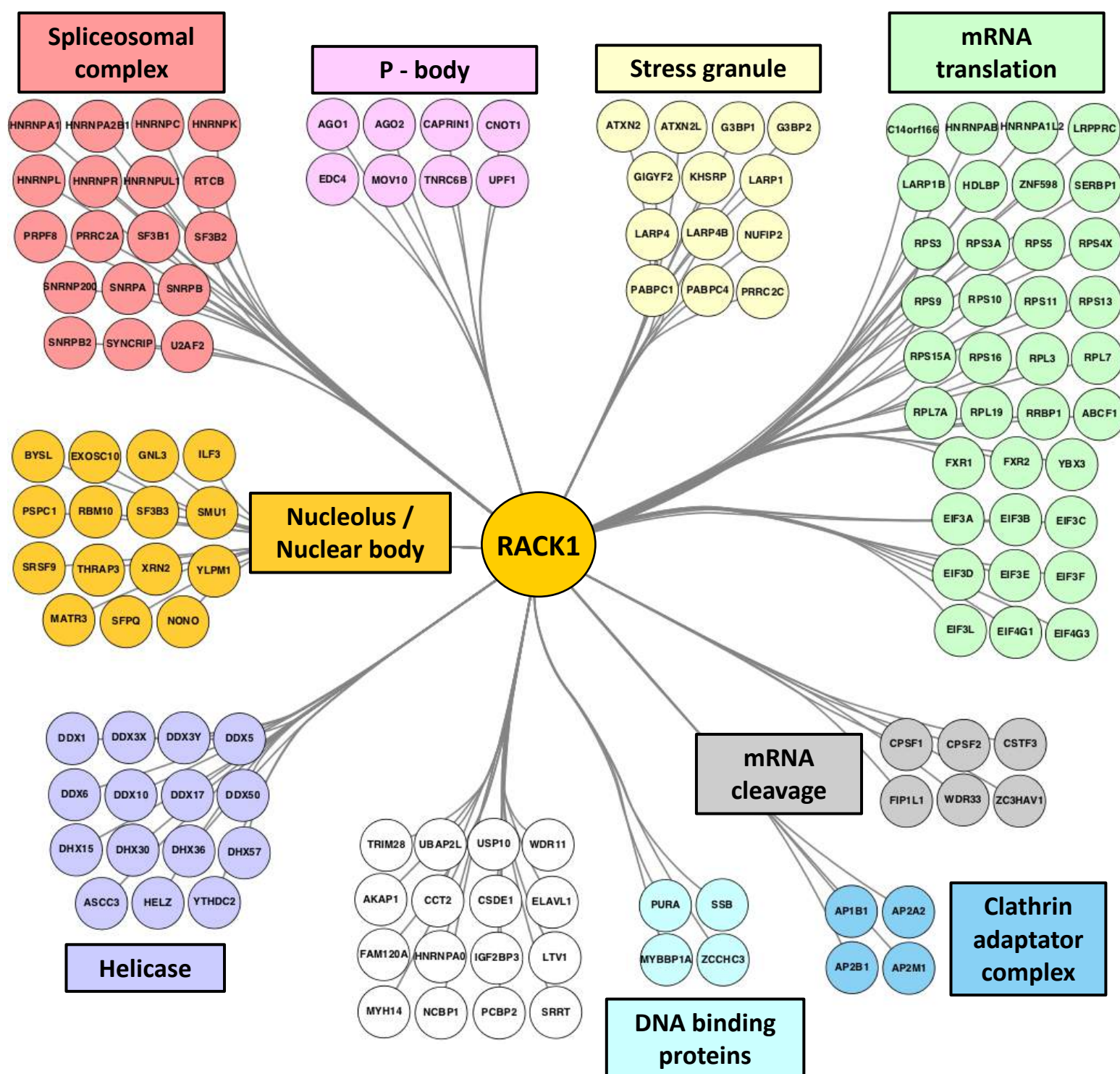


Figure 2

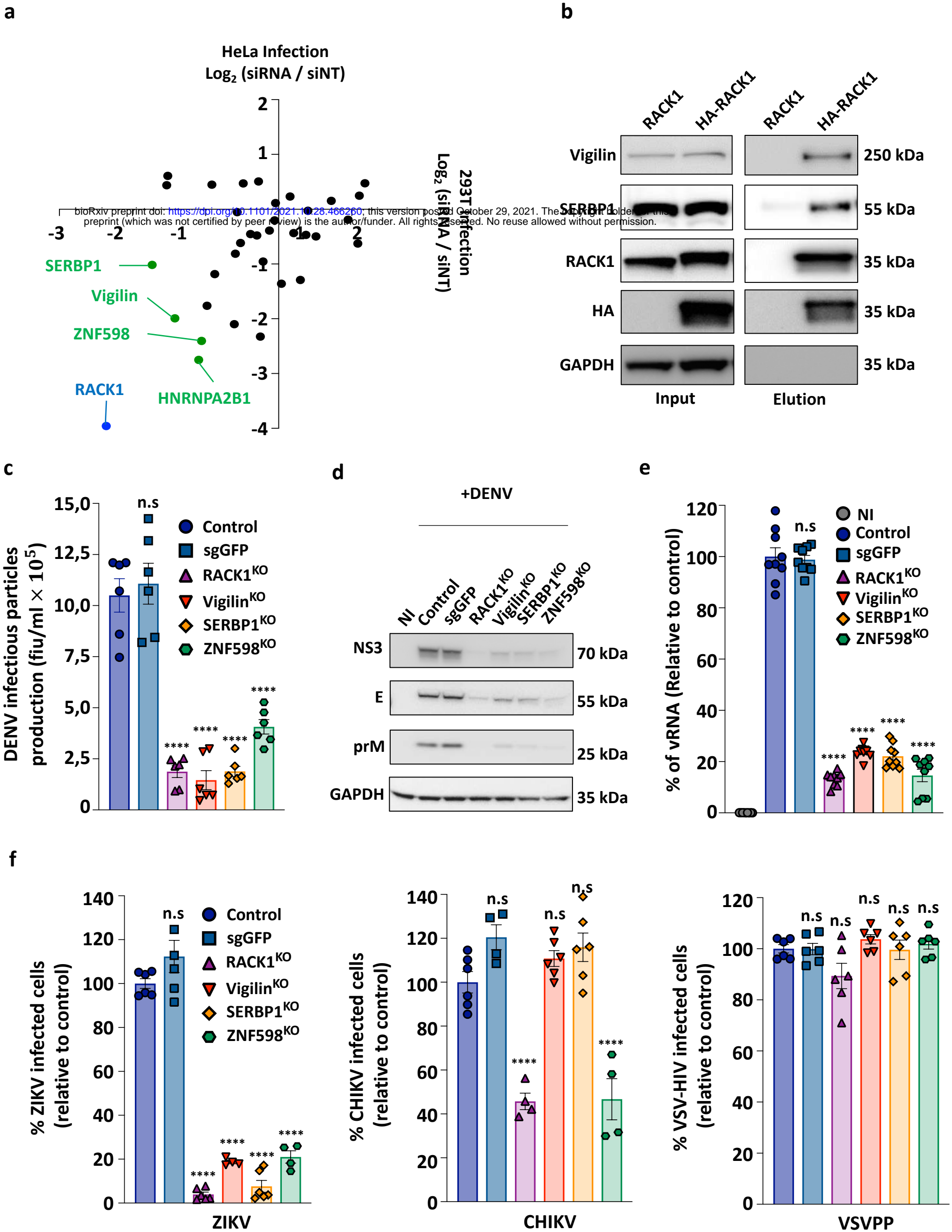
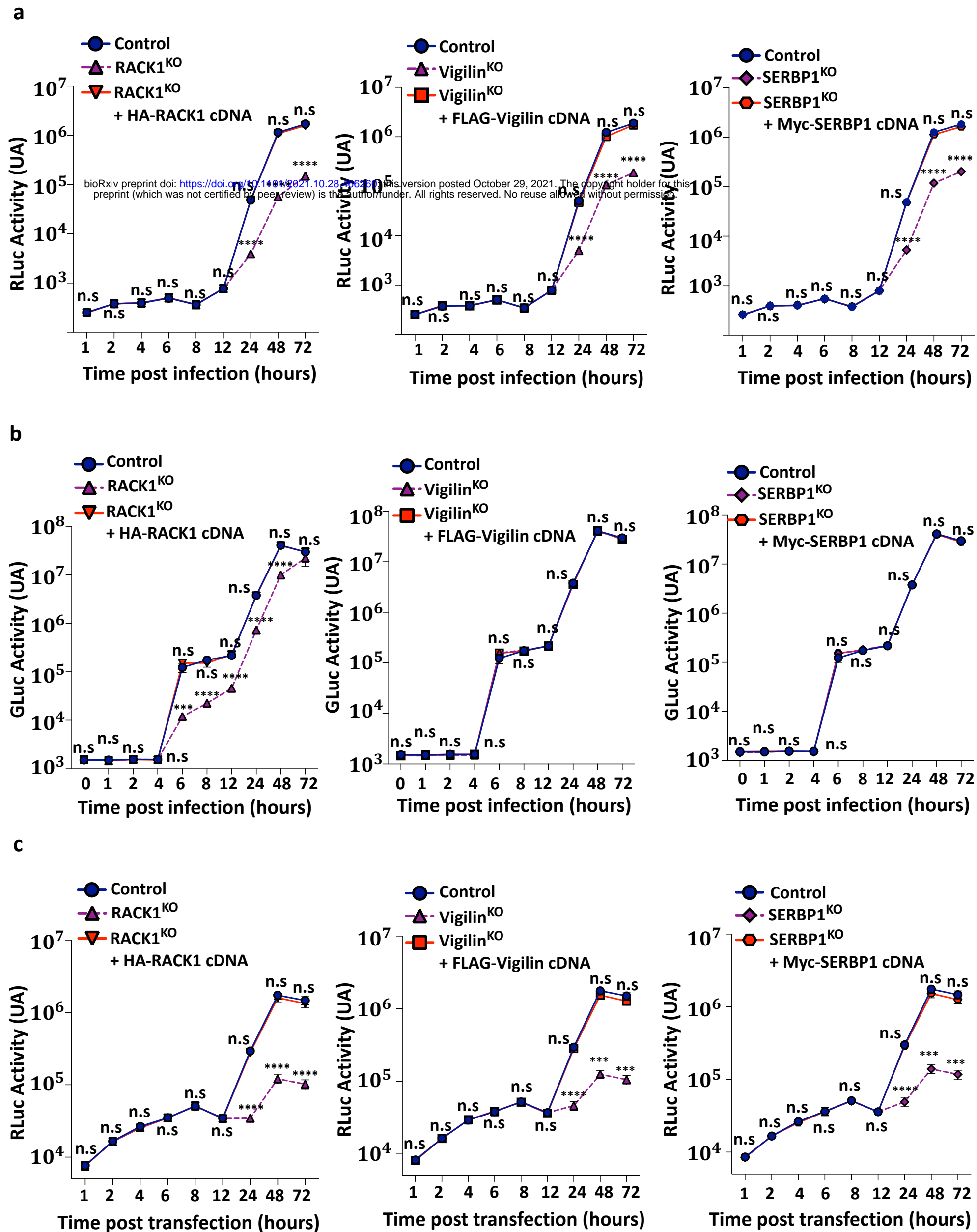
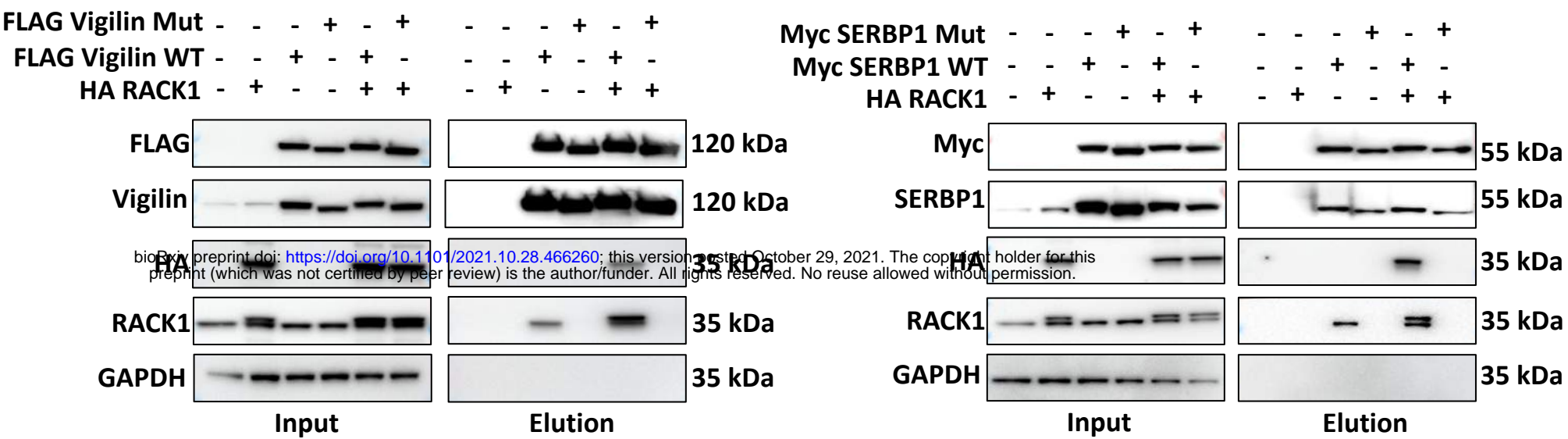


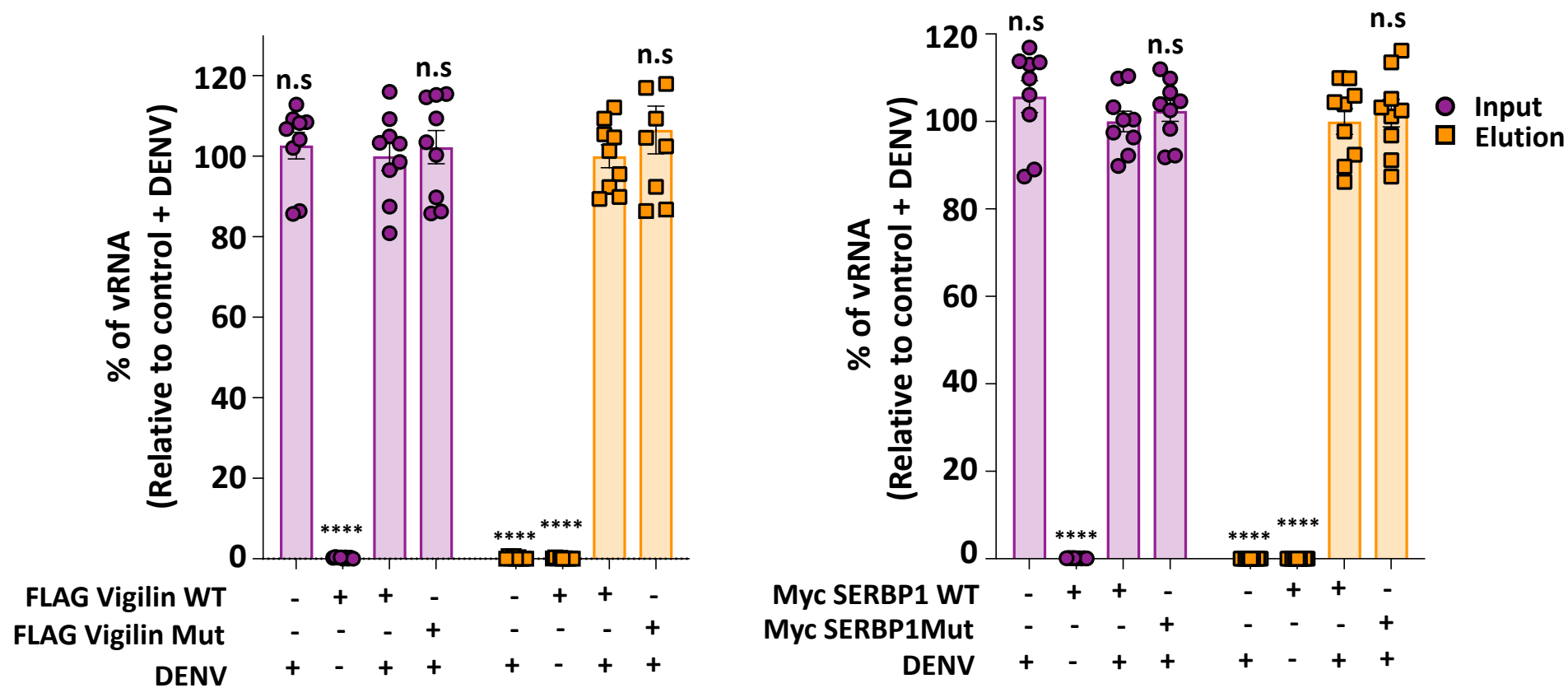
Figure 3



a



b



c

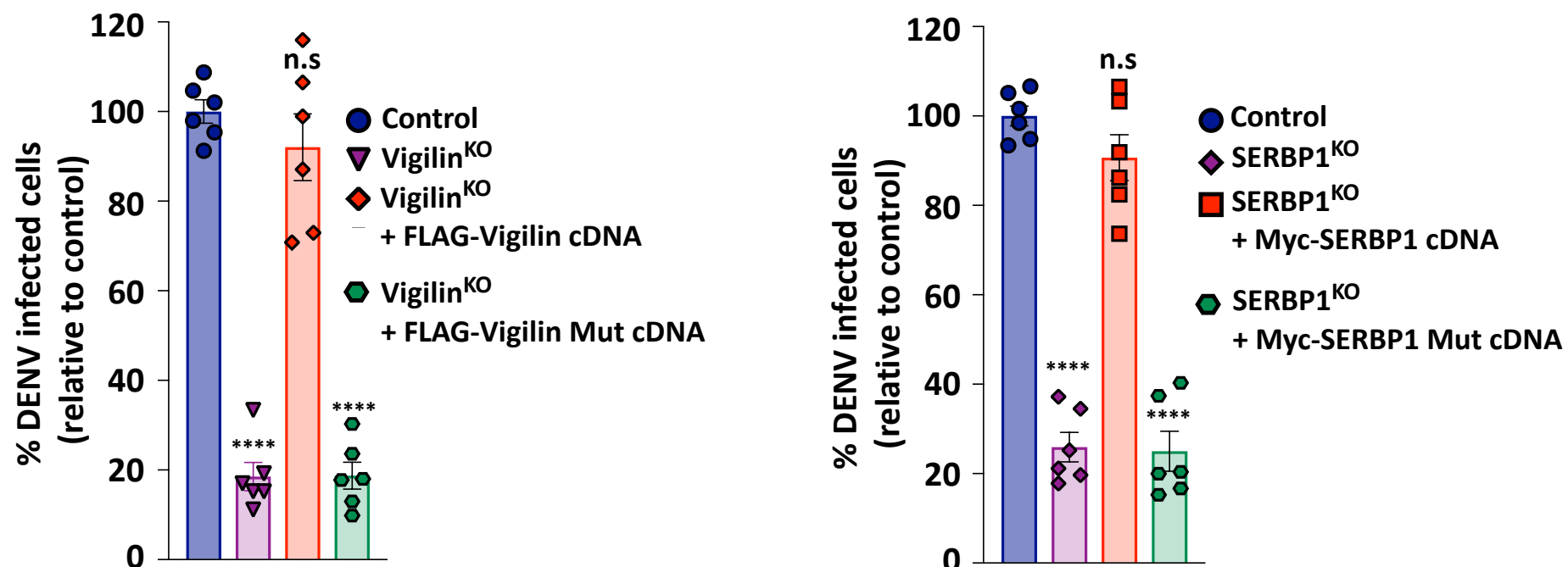


Figure 5